HHS Public Access

Author manuscript

Mol Carcinog. Author manuscript; available in PMC 2017 May 01.

Published in final edited form as:

Mol Carcinog. 2016 May ; 55(5): 600–610. doi:10.1002/mc.22306.

Antagonizing Pathways Leading to Differential Dynamics in Colon Carcinogenesis in Shugoshin1 (Sgo1)-Haploinsufficient Chromosome Instability Model

Chinthalapally V. Rao[1], **Saira Sanghera**[2], **Yuting Zhang**[1], **Laura Biddick**[1], **Arun Reddy**[1], **Stan Lightfoot**[1], **Wei Dai**[3], and **Hiroshi Y. Yamada**[1]

[1] Center for Cancer Prevention and Drug Development, Department of Medicine, Hematology/Oncology Section, University of Oklahoma Health Sciences Center (OUHSC), Oklahoma City, OK

[2] College of Arts & Sciences, Baylor University, Waco, TX

[3] Department of Environmental Medicine, New York University Langone Medical Center, Tuxedo, NY

Abstract

Colon cancer is the second most lethal cancer. It is predicted to claim 50,310 lives in 2014. Chromosome Instability (CIN) is observed in 80-90% of colon cancers, and is thought to contribute to colon cancer progression and recurrence. However, there are no animal models of CIN that have been validated for studies of colon cancer development or drug testing. In this study, we sought to validate a mitotic error-induced CIN model mouse, the Shugoshin1 (Sgo1) haploinsufficient mouse, as a colon cancer study model. Wild-type and $Sgo1^{-/+}$ mice were treated with the colonic carcinogen, azoxymethane (AOM). We tracked colon tumor development 12, 24, and 36 weeks after treatment to assess progression of colon tumorigenesis. Initially, more precancerous lesions, Aberrant Crypt Foci (ACF), developed in $Sgo1^{-/+}$ mice. However, the ACF did not develop straightforwardly into larger tumors. At the 36-week endpoint, the number of gross tumors in $Sgo1^{-/+}$ mice was no different from that in wild-type controls. However, Copy Number Variation (CNV) analysis indicated that fully developed colon tumor in $Sgo1^{-/+}$ mice carried 13.75 times more CNV. Immunohistological analyses indicated that $Sgo1^{-/+}$ mice differentially expressed IL-6, Bcl2, and $p16^{INK4A}$. We propose that formation of ACF in $Sgo1^{-/+}$ mice is facilitated by the IL6-STAT3-SOCS3 oncogenic pathway and by the Bcl2-anti-apoptotic pathway, yet further development of the ACF to tumors is inhibited by the $p16^{INK4A}$ tumor suppressor pathway. Manipulating these pathways would be beneficial for inhibiting development of colon cancer with CIN.

Keywords

Sgo1 (Shugoshin 1); mice; Colon cancer; Azoxymethane (AOM); Chromosome Instability (CIN)

Corresponding Authors Hiroshi Y. Yamada (Hiroshi-yamada@ouhsc.edu, Tel: 405-271-3224 ext 32524), Chinthalapally V. Rao (cv-rao@ouhsc.edu, Tel: 405-271-3224) Department of Medicine, Hem/Onc Section, University of Oklahoma Health Sciences Center (OUHSC), 975 NE 10th St. BRC1207, Oklahoma City, Oklahoma 73104 Fax 405-271-3225.

Introduction

Colorectal cancer is the second most lethal cancer in the U.S. The American Cancer Society predicts 50,310 deaths from colorectal cancer in 2014 (1). Various factors, including age, environmental factors, smoking habits, diet, and genetic predispositions such as a mutation in tumor suppressor *Adenomatous Polyposis Coli (apc)*, play major roles in colorectal cancer development. Increased Chromosome Instability (CIN) is a prevailing biological trait of colon cancer. Eighty to ninety percent of human colon cancer is associated with high CIN, which far exceeds the Microsatellite Instability (MIN) observed in approximately 15% (2).

Studies demonstrated that CIN plays a critical role in cancer progression and, perhaps, in initiation (3-5). High CIN may also increase the rate of relapse, leading to poor prognosis (6). Tumor mass-sequencing revealed that human colon cancers have several sets of frequently mutated genes and corresponding pathways, including PI3K, KRAS, APC, TP53, FBXW7, and chromosome cohesion (7-9). *In vitro* manipulation of these genes results in elevated CIN (10-15), suggesting that the normal functions of these genes include prevention of CIN (16). Once the high CIN condition is introduced, accelerated chromosome loss leading to loss of heterozygosity (LOH) of tumor suppressors can occur. Also chromosome gain and oncogene activation contributing to tumorigenesis can occur, although detailed entire genome analysis studies are rare (17). Since *apc* mutation is an early event in human colonic carcinogenesis (18), CIN begins early in carcinogenesis. With additional mutations, the degree of CIN increases, accelerating further mutations. With feedback-type effects, CIN is a critical phenotype that must be addressed as anti-cancer measures are developed (16).

The current development of colon cancer drugs depends on a set of animal models that each have a specific focus, including: (i) wild-type animals treated with a chemical carcinogen (e.g., AOM), (ii) wild-type animals treated with a chemical carcinogen and inflammatory reagent (e.g., DSS; AOM-DSS colitis model), (iii) transgenic $apc^{min/+}$ mice that mimic prevailing mutations in *apc*, and (iv) transgenic Msh2 and Msh3 mice that represent mutations causing MIN (19-20). Each animal model, an essential bridge to human trials, reflects a specific aspect of carcinogenesis. Thus, the usefulness of each animal model is limited within the scope of the particular model. For this reason, we need a new animal model that characterizes previously under-represented aspects of colonic carcinogenesis. Once such a model is validated and introduced to the drug assessment system, it will help researchers to identify effective treatments for human populations that have thus far been non-responsive to existing drugs, due to differences in the molecular causes of their cancers.

In recent years, researchers have developed new transgenic mouse models targeting mitotic processes, such as the mitotic spindle checkpoint (21). These models have received recognition as excellent study models for certain cancers, with well-defined defects in biological processes (22-25). As a part of these efforts, Shugoshin 1 (Sgo1) haploinsufficient model mice were established (26-29). Evidence suggests that Sgo1 and the chromosome cohesion pathway is involved in colon cancer (9, 29, 30).

Sgo1 is a centromeric protein, protecting chromosome-tethering cohesin proteins from premature degradation during mitosis, thus maintaining mitotic chromosome cohesion

(26-31). Reduced amounts of Sgo1 result in chromosome cohesion defects and elevated CIN (15, 28, 29). Studies by us and others showed that Sgo1 affects centrosomal function, and that the defect leading to multipolar cell division leads to CIN (29, 31).

In the present study, building upon our previous work that showed the rapid development of colon lesions and micro-tumors (29), we sought to validate $Sgo1^{-/+}$ haploinsufficient mice as a new model for colon cancers that are aggravated by high CIN. Unexpectedly, early colonic lesions and microadenomas in $Sgo1^{-/+}$ did not develop into larger tumors in a straightforward manner. However, we observed that a tumor in Sgo1 animals had 13.75 times more CNV than a tumor in control animals. We identified antagonizing oncogenic and tumor-suppressing pathways that are differentially expressed in $Sgo1^{-/+}$ mice and may be responsible for the different dynamics in colon cancer development.

Materials and Methods

Animals and AOM treatments

$Sgo1^{-/+}$ mice were generated and maintained in the OUHSC Biomedical Research Center rodent barrier facility (26, 29). We bred forty-five female wild-type mice and forty-five female $Sgo1^{-/+}$ mice. All mice were generated with the low-cancer-susceptible C57BL/6 background. Standard diet (Purina) was fed throughout the experiment. On the 7th week after birth, the mice were grouped. Beginning in the 8th week, all mice were intraperitoneally injected with 4 mg/kg AOM diluted in 0.9% saline, twice a week for four weeks (8 administrations in total). We euthanized 15 wild-type mice and 15 $Sgo1^{-/+}$ mice using CO_2 asphyxiation at three different time points: the 12th, 24^{th}, and 36th weeks after completion of AOM treatment. At each end point, we performed necropsies with gross examinations for tumors and any abnormalities. From 7 mice from each group, we collected normal-looking colonic mucosal tissue by scraping. Visible tumors were collected separately. The scraped colonic mucosal tissues and tumors were snap-frozen in liquid nitrogen, and stored in a −80°C freezer. From 8 mice from each group, colons were cut open longitudinally and fixed in 10% formalin for ACF and tumor counting. ACF were counted with methylene blue staining and bright field microscopy (29). Visible tumors were recorded and confirmed by a histopathologist after paraffin embedding. All treatments were in compliance with protocols approved by the OUHSC institutional animal care and use committee.

Immunohistochemistry (IHC) and immunoblots

Once the ACF counting was completed, we embedded the colons in paraffin and made sections with a microtome (OUHSC Advanced Immunohistochemistry & Morphology Core Facility). We used the sections for Hematoxylin/Eosin (H/E) staining and for IHC (Histostain SP kit or SuperPicture 3rd Gen IHC kit, Invitrogen). The following primary antibodies were used at 1.0 μg/ml: anti-$p16^{INK4A}$ (Lifespan Biosciences, LS-B1347), anti-p53 (Santa Cruz Biotechnology, SC-6243), anti-Bax (biorbyt, orb4655), anti-Bcl2 (Santa Cruz Biotechnology, SC-492), anti-Bclxl (biorbyt, orb10175), anti-COX2 (Thermo Scientific, PA5-16817), anti-IL6 (Abcam, ab6672), anti-PCNA (biorbyt, orb11248), anti-phospho-H2AX (γ-H2AX, Novus Biologicals, Catalog No. NBP-1-19931), and anti-Sgo1

(SGOL1; Proteintech, 16977-1-AP). IHC images were captured with a microscope with a CCD camera (Olympus) from at least seven mice for each strain. These immunohistochemical stains were graded on a semi-quantitative seven-point scale according to the prevalence and intensity of stain in the cells of overall normal-looking part of colon tissues: 1: no staining (0%), 2: weak stain in 1-5%, 3: weak stain in 5-20%, alternatively moderate/strong stain in 5-10%, 4: weak stain in 20-60%, alternatively, moderate/strong stain in 10-35%, 5: weak stain in >60%, alternatively moderate/strong stain in 35-50%, 6: moderate/strong stain in 50-75%, 7: strong stain in >75%.

Standard immunoblotting procedures were followed as previously described (32). Colonic mucosal tissues were extracted in extraction buffer with homogenizer, then boiled with SDS loading buffer for 5 minutes. Protein concentration was quantified using protein assay dye reagent (Biorad) and equalized. Immune complexes were detected with appropriate secondary antibodies conjugated with horseradish peroxidase (Sigma) and with chemiluminescence reagents (Thermo Scientific)

Statistics

Data were expressed as means ± *SD*, or as variances. The differences between groups were analyzed using Student's t-test with Graphpad Prism5 software.

Copy Number Variation (CNV) analysis

All samples were collected at endpoint 3 (36^{th} week). Pooled normal-looking mucosal tissues from wild-type (n=6) and Sgo1 (n=6) animals, and colon tumors from wild-type (n=1) and Sgo1 (n=1) animals (both groups developed only one 3mm+ size tumor usable for CNV) were sent to Miltenyi Biotec (Auburn, CA) for genomic DNA extraction followed by array-based Comparative Genomic Hybridization for CNV analysis (4x180k). Detailed data were uploaded as supplemental data.

Next Generation Sequencing (NGS)

We isolated messenger RNA from normal-looking mucosal tissues collected from wild-type (n=6) and Sgo1 (n=6) animals at endpoint 2 (24^{th} week) using a Totally RNA kit (Ambion) followed by a PolyA purist mRNA purification kit (Ambion). The resulting 12 samples were sent to the OUHSC Laboratory for Molecular Biology and Cytometry Research core facility (Microgen) for NGS. The NGS readouts were uploaded to Geospiza company server and analyzed with Genesifter software. Mapped reads were used for equalization. Statistical significance was evaluated with Student's t-test.

Results

The primary objective of this study was to validate the role of Sgo1 haploinsufficiency as a CIN model of colon cancer. Colon cancer model mice should meet two criteria: (i) show increased rates of colonic Aberrant Crypt Foci (ACF), adenoma, and/or adenocarcinoma, and (ii) show progression from ACF to adenoma/adenocarcinoma over a reasonable length of time for laboratory experiments (e.g., 36-48 weeks). In a previous study with an endpoint 12 weeks after completion of AOM treatments, we observed that the $Sgo1^{-/+}$ mice met the

first criterion (29), and anticipated that the ACF would grow to tumors in Sgo1$^{-/+}$ mice. In the current project, we extended the time course of the analysis and tested whether the animals met the second criterion (Fig 1A). We observed that the average body weights were comparable between the control and Sgo1$^{-/+}$ mice throughout the experiment (Fig 1B). Unexpectedly, there was no significant difference in the numbers of gross tumors in the control and Sgo1$^{-/+}$ mice (Table 1; colonic tumor counts). The results obtained at the 24th and 36th weeks after the completion of AOM treatments did not support our prediction that Sgo1$^{-/+}$ mice would develop more tumors than the control animals.

To investigate the reason, we first counted ACF and micro-tumors (adenomas) to monitor the dynamics of colon tumor development in Sgo1$^{-/+}$ and control mice. At the first endpoint (12 weeks), we observed more ACF and micro-tumors in Sgo1$^{-/+}$ mice, consistent with the previous results (29; Fig 2A). At the second endpoint (24 weeks; Fig 2B), we observed fewer total ACF in Sgo1$^{-/+}$ mice than in controls ($p<0.05$), suggesting a rapid regression of the ACF observed earlier in Sgo1$^{-/+}$ mice. At the third endpoint (36 weeks; Fig 2C), most ACFs had regressed in both strains, and we observed comparable numbers of micro and larger colon tumors in Sgo1$^{-/+}$ mice and controls. Overall, the rapid development of ACF and micro tumors in Sgo1$^{-/+}$ mice at the early endpoint (12 weeks) did not translate into an increase in the development of larger or additional colon tumors.

To explain the differential development of ACF and colon tumors between Sgo1$^{-/+}$ CIN mice and the controls, and to answer why the development of ACFs did not translate to tumor development, we hypothesized that Sgo1$^{-/+}$ mice differentially express a set of genes that influence oncogenic or tumor-suppressing processes. To test the hypothesis, we performed immunohistochemistry experiments for following ten marker proteins: proliferation and growth (PCNA), cancer (p53), inflammation (COX-2, IL-6), DNA damage (phospho-HistoneH2AX), cell death (Bcl2, Bcl-xl, Bax), and senescence (p16^{INK4A}, p21^{WAF1}) in normal-looking and cancerous tissues in Sgo1$^{-/+}$ and wild-type mice. The IHC signal was graded in a seven point-scale (see Materials and Methods). More than 1 average scale difference was judged as differentially expressed (n=6~8; Figure 3, asterisk).

During the early stages (12 weeks) when Sgo1$^{-/+}$ mice showed quick development of ACF, we observed an increase in cytokine IL-6 and apoptosis regulator Bcl2, as documented in our previous study (29). We considered them to be candidate factors for the accelerated lesion formation. At the midpoint (24 weeks) when Sgo1$^{-/+}$ mice showed an unexpected reduction in ACF development, we observed a notable difference in the IHC signals in three markers: IL-6, Bcl2, and tumor suppressor p16^{INK4A}. At the late stage (36 weeks), we observed a difference in Bcl2, BclxL, Bax, IL-6, and p21^{WAF1}, another tumor suppressor.

We questioned whether the expression difference correlated with the development of lesions and tumors. For this purpose, we focused on endpoint 2 (24 weeks), when ACF reduction was most notable. IL-6 expression was generally low in normal-looking mucosa in both Sgo1$^{-/+}$ and control animals, but higher in lesions in Sgo1$^{-/+}$ animals (Fig 4A). In contrast, Bcl2 expression was higher in normal-looking parts of colons in Sgo1$^{-/+}$ than in controls. As lesions developed, Bcl2 expression increased (Fig 4B). p16^{INK4A} is a bona-fide tumor suppressor, and p16^{INK4A} expression was low in wild-type mice, but higher in Sgo1$^{-/+}$ mice,

both in normal-looking colons and in lesions. Thus the tumor suppression in Sgo1$^{-/+}$ mice model can be explained through the p16 behavior at least in part (Fig 4C).

Immunoblots from endpoint 2 (Fig 4D) supported the IHC results, showing activation of the IL-6-STAT3-SOCS3 pathway, and increases in Bcl2, Bax, and p16 ^{INK4A}. However, NGS results indicated that the messenger RNA levels were not significantly changed (Fig 4E), suggesting that the protein accumulations may be mediated post-transcriptionally rather than transcriptionally.

At endpoint 3, we observed limited numbers of gross colon tumors in both wild-type and Sgo1 mice (Table 1), and questioned the impact of Sgo1 haploinsufficiency on the tumors in Sgo1. CIN was theorized to increase DNA damage, whole chromosome loss and gain, and Copy Number Variation (CNV), although the theory has not been fully substantiated. Using the tumors and normal-looking colonic mucosal tissues, we performed CNV analysis with comparative genomic hybridization (Miltenyi Biotec; Fig 5). When compared with normal-looking mucosa in wild-type animals, the tumor in wild-type animal had 12 CNV (Fig 5A). However, when normal-looking mucosa in Sgo1 animals was compared with the tumor in Sgo1 animal, the tumor in Sgo1 had 165 CNV (Fig 5B). Thus, the tumor CNV was 13.75 times higher in Sgo1 mice than in wild-type mice. This is a clear demonstration that tumors with Sgo1 haploinsufficiency can develop high CNV, as theorized. The comparison between tumors in wild-type and in Sgo1 mice indicated 40 CNV (Fig 5C), demonstrating that the tumor in Sgo1 mice had additional genomic alterations compared with the tumors in wild-type mice.

Almost all CNV in the Sgo1 tumor were amplification/gain (163 among 165; Fig 5B), indicating a strong preference for genomic gain and bias against loss in this particular model. Some genes with CNV have been shown to be involved in or associated with carcinogenesis in the GI tract, including amplifications of proto-oncogene Src (Src; 33), Mitogen-Activated Protein Kinase Kinase 2 (Map2k2; 34), and cyclinD2 (Ccnd2; 35) (Supplemental data). Amplification in these genes may have directly or indirectly contributed to tumorigenesis in Sgo1$^{-/+}$ mice.

Discussion

In our previous study (29), the results of which were confirmed in this study, we observed increased ACF and micro tumors 12 weeks after AOM treatments in Sgo1$^{-/+}$ CIN model mice. We anticipated that the increase would translate into enhanced colonic tumor progression over time. However, to our surprise, numbers of colonic tumors were comparable between Sgo1$^{-/+}$ and control animals, indicating that ACF did not straightforwardly develop into tumors in the Sgo1$^{-/+}$ mice.

We also found an increase in IL-6 and Bcl2 in our previous work, and suggested that these increases might contribute to rapid development of ACF and tumors. We also observed IL-6 and Bcl2 increases at later endpoints in the present study, suggesting that increased IL-6 and Bcl2 are consistent characteristics of the colonic tissues of Sgo1$^{-/+}$ mice, and may possibly be drivers for carcinogenesis.

Activation of the IL-6-STAT3-SOCS3 pathway can facilitate development of colon cancer. IL-6 is a reliable serum marker for colon cancer (36). IL-6 activates transcription factors, including STAT3, via phosphorylation; in myeloma cells, constitutively activated STAT3 confers resistance to apoptosis through Bcl-xL expression (37). As compared to healthy subjects, patients with active ulcerative colitis, who are prone to develop colon cancer, had significantly more IL-6- and phospho-STAT3-positive epithelial cells (38). High CIN correlates with IL-6 DNA amplification in the human colon (39).

Increased Bcl2 is also implicated in colon cancer development. Increased Bcl2 generally inhibits apoptosis and aids survival of cells via interference with the Bcl2-Bax-mitochondrial cell death pathway. Bax (Bcl2 associated X protein) was upregulated and Bcl-2 was downregulated after selenium treatment for colon cancer cell lines, suggesting that decreased Bcl2 aids selenium-mediated chemoprevention of colon cancer (40). A major colon cancer signaling component, beta-catenin, induced c-Myc, E2F1, and Bcl-2 as its downstream target in rats (41).

How does Sgo1 haploinsufficiency, or an increase of CIN, lead to increased expressions of IL-6 and Bcl2? A possible link is DNA damage in high CIN tissue. CIN is known to increase cellular DNA damage (42, 43). In human primary monocytes, IL-6 production is increased with DNA damage (44). The hypothesis that DNA damage is an inducer of IL-6 in colonic mucosal tissue under high CIN conditions is untested. Perhaps due to the limited number of CIN-influenced mitotic cells in the tissue, straightforward IHC and immunoblots did not show a notable increase in DNA damage markers (Fig 3 IHC for γH2AX; blots not shown). Thus, better tracking systems may be needed. Alternatively, colonic cells with CIN may acquire the ability to induce IL-6 expression in surrounding fibroblasts, as colon cancer cells can (45).

Another question is why $Sgo1^{-/+}$ mice did not promote ACFs' progression to colonic tumors at later stages than wild-type controls. We identified a candidate pathway: senescence mediated by $p16^{INK4A}$. $p16^{INK4A}$ is a major tumor suppressor for colon tumors. p16 is frequently mutated or epigenetically silenced in colon cancer (46, 47). Consistent with the idea that CIN induces senescence, mice with a hypomorphic allele of BubR1, a spindle checkpoint component defect which also leads to CIN, show premature aging that is at least partly dependent on $p16^{INK4A}$ (48, 49). Thus, the tumorigenic effects of CIN could be actively counteracted by senescent proteins *in vivo*.

Overall, $Sgo1^{-/+}$ lesions may develop rapidly with activation of the IL-6 pathway. In addition, normal-looking tissues in $Sgo1^{-/+}$ animals may have activated an anti-apoptotic pathway, and may be resistant to apoptosis-based tumor suppression. These may contribute to rapid development of early lesions. However, the $p16^{INK4A}$-dependent tumor suppressing pathway is also activated in $Sgo1^{-/+}$ tissues, both in normal-looking parts of colons and in lesions. This would explain the lack of further development of lesions into later stage tumors in $Sgo1^{-/+}$ mice. CIN and resulting aneuploidy acts both oncogenically and as a tumor suppressor in an organ-specific manner (22-25, 50). Our study adds further explanation to the phenomenon.

At the late stage (36 weeks), we observed a limited number of colon tumors. To characterize the developed tumors, we performed CNV analysis and observed a difference in CNV at a greater than 10 times magnitude in analyzed tumors (Fig 5). This result was striking, although the sample numbers obtained in this experiment were not large enough to statistically conclude that there is a heavier CNV burden in Sgo1 tumors. CNV analysis with larger tumor sample sets is warranted to further determine the effect of CIN on CNV and tumor development, and possibly identify frequent CNV sites that are specific to tumors with Sgo1 defects.

In this study, we attempted to validate $Sgo1^{-/+}$ CIN mice as a novel colon tumor study model, and unexpectedly showed the complexity of CIN involvement in colonic carcinogenesis. Our results suggest that CIN can alter protein expressions in tissues, which may lead to differential dynamics of colon cancer development. With further study, this differential protein expression may be exploited for selective eradication of CIN cells, or modulation of the development of colon cancer with high CIN for therapeutic and/or chemoprevention purposes such as through IL-6 inhibitor.

Supplementary Material

Refer to Web version on PubMed Central for supplementary material.

Acknowledgements

We thank Mrs. Kathy J. Kyler for editing the manuscript. We want to thank the OUHSC Rodent Barrier Facility animal care technical staff for the help in maintenance of mice.

Financial support

This work was supported by grants from the US National Institutes of Health to C.V.R (NCI R01CA094962), W.D. (RO1CA090658), and H.Y.Y (NCI RO3CA162538); also supported by a Chris4Life colon cancer foundation pilot study grant to H.Y.Y.

List of Abbreviations

ACF	Aberrant Crypt Foci
AOM	Azoxymethane
APC	Adenomatous Polyposis Coli
Bax	Bcl-associated X protein
Bcl2	B cell lymphoma 2
CIN	Chromosome Instability
CNV	Copy Number Variations
DSS	Dextran Sodium Sulfate
FBXW7	F-box/WD repeat-containing protein 7
H2AX	Histone H2A member X

IHC	Immunohistochemistry
IL-6	Interleukin 6
MIN	Microsatellite Instability
NGS	Next Generation Sequencing
PCNA	Proliferating Cell Nuclear Antigen
PI3K	Phosphoinositide 3-Kinase
Sgo1	Shugoshin 1
SOCS3	Suppressor of Cytokine Signaling 3
STAT3	Signal Transducer And Activator of Transcription 3
TP53	Tumor Protein p53

References

1. American Cancer Society (ACS) statistics for colon cancer. 2014. http://www.cancer.org/cancer/colonandrectumcancer/detailedguide/colorectal-cancer-key-statistics
2. Dunican DS, McWilliam P, Tighe O, Parle-McDermott A, Croke DT. Gene expression differences between the microsatellite instability (MIN) and chromosomal instability (CIN) phenotypes in colorectal cancer revealed by high-density cDNA array hybridization. Oncogene. 2002; 21(20): 3253–7. [PubMed: 12082642]
3. Holland AJ, Cleveland DW. Boveri revisited: chromosomal instability, aneuploidy and tumorigenesis. Nat Rev Mol Cell Biol. 2009; 10(7):478–87. [PubMed: 19546858]
4. Tanaka K, Hirota T. Chromosome segregation machinery and cancer. Cancer Sci. 2009; 100(7): 1158–65. [PubMed: 19432891]
5. Chandhok NS, Pellman D. A little CIN may cost a lot: revisiting aneuploidy and cancer. Curr Opin Genet Dev. 2009; 19(1):74–81. [PubMed: 19195877]
6. Sotillo R, Schvartzman JM, Socci ND, Benezra R. Mad2-induced chromosome instability leads to lung tumour relapse after oncogene withdrawal. Nature. 2010; 464(7287):436–40. [PubMed: 20173739]
7. Wood LD, Parsons DW, Jones S, Lin J, Sjöblom T, Leary RJ, et al. The genomic landscapes of human breast and colorectal cancers. Science. 2007; 318(5853):1108–13. [PubMed: 17932254]
8. Chittenden TW, Howe EA, Culhane AC, Sultana R, Taylor JM, Holmes C, et al. Functional classification analysis of somatically mutated genes in human breast and colorectal cancers. Genomics. 2008; 91(6):508–11. [PubMed: 18434084]
9. Barber TD, McManus K, Yuen KW, Reis M, Parmigiani G, Shen D, et al. Chromatid cohesion defects may underlie chromosome instability in human colorectal cancers. Proc Natl Acad Sci U S A. 2008; 105(9):3443–8. [PubMed: 18299561]
10. Liu W, Zhou Y, Reske SN, Shen C. PTEN mutation: many birds with one stone in tumorigenesis. Anticancer Res. 2008; 28(6A):3613–19. [PubMed: 19189642]
11. Castagnola P, Giaretti W. Mutant KRAS, chromosomal instability and prognosis in colorectal cancer. Biochim Biophys Acta. 2005; 1756(2):115–125. [PubMed: 16112461]
12. Dikovskaya D, Schiffmann D, Newton IP, Oakley A, Kroboth K, Sansom O, et al. Loss of APC induces polyploidy as a result of a combination of defects in mitosis and apoptosis. J Cell Biol. 2007; 176(2):183–195. [PubMed: 17227893]
13. Rusan NM, Peifer M. Original CIN: reviewing roles for APC in chromosome instability. J Cell Biol. 2008; 181(5):719–726. [PubMed: 18519734]

14. Tomasini R, Mak TW, Melino G. The impact of p53 and p73 on aneuploidy and cancer. Trends Cell Biol. 2008; 18(5):244–252. [PubMed: 18406616]
15. McGuinness BE, Hirota T, Kudo NR, Peters JM, Nasmyth K. Shugoshin prevents dissociation of cohesin from centromeres during mitosis in vertebrate cells. PLoS Biol. 2005; 3(3):e86. [PubMed: 15737064]
16. Rao CV, Yamada HY. Genomic instability and colon carcinogenesis: from the perspective of genes. Front Oncol. 2013; 3:130. [PubMed: 23734346]
17. Baker DJ, Jin F, Jeganathan KB, van Deursen JM. Whole chromosome instability caused by Bub1 insufficiency drives tumorigenesis through tumor suppressor gene loss of heterozygosity. Cancer Cell. 2009; 16(6):475–86. [PubMed: 19962666]
18. Fearon ER, Vogelstein B. A genetic model for colorectal tumorigenesis. Cell. 1990; 61(5):759–67. [PubMed: 2188735]
19. Taketo MM, Edelmann W. Mouse models of colon cancer. Gastroenterology. 2009; 136(3):780–98. [PubMed: 19263594]
20. Rosenberg DW, Giardina C, Tanaka T. Mouse models for the study of colon carcinogenesis. Carcinogenesis. 2009; 30(2):183–96. [PubMed: 19037092]
21. Rao CV, Yang YM, Swamy MV, Liu T, Fang Y, Mahmood R, et al. Colonic tumorigenesis in BubR1+/-ApcMin/+ compound mutant mice is linked to premature separation of sister chromatids and enhanced genomic instability. Proc Natl Acad Sci U S A. 2005; 102(12):4365–70. [PubMed: 15767571]
22. Rao CV, Yamada HY, Yao Y, Dai W. Enhanced genomic instabilities caused by deregulated microtubule dynamics and chromosome segregation: a perspective from genetic studies in mice. Carcinogenesis. 2009; 30(9):1469–74. [PubMed: 19372138]
23. Foijer F, Draviam VM, Sorger PK. Studying chromosome instability in the mouse. Biochim Biophys Acta. 2008; 1786(1):73–82. [PubMed: 18706976]
24. Ricke RM, van Ree JH, van Deursen JM. Whole chromosome instability and cancer: a complex relationship. Trends Genet. 2008; 24(9):457–66. [PubMed: 18675487]
25. Schvartzman JM, Sotillo R, Benezra R. Mitotic chromosomal instability and cancer: mouse modelling of the human disease. Nat Rev Cancer. 2010; 10(2):102–15. [PubMed: 20094045]
26. Wang X, Yang Y, Duan Q, Jiang N, Huang Y, Darzynkiewicz Z, et al. sSgo1, a major splice variant of Sgo1, functions in centriole cohesion where it is regulated by Plk1. Dev Cell. 2008; 14(3):331–41. [PubMed: 18331714]
27. Wang X, Dai W. Shugoshin, a guardian for sister chromatid segregation. Exp Cell Res. 2005; 310(1):1–9. [PubMed: 16112668]
28. Salic A, Waters JC, Mitchison TJ. Vertebrate shugoshin links sister centromere cohesion and kinetochore microtubule stability in mitosis. Cell. 2004; 118(5):567–78. [PubMed: 15339662]
29. Yamada HY, Yao Y, Wang X, Zhang Y, Huang Y, Dai W, et al. Haploinsufficiency of SGO1 results in deregulated centrosome dynamics, enhanced chromosomal instability and colon tumorigenesis. Cell Cycle. 2012; 11(3):479–88. [PubMed: 22262168]
30. Iwaizumi M, Shinmura K, Mori H, Yamada H, Suzuki M, Kitayama Y, et al. Human Sgo1 downregulation leads to chromosomal instability in colorectal cancer. Gut. 2009; 58(2):249–60. [PubMed: 18635744]
31. Schöckel L, Möckel M, Mayer B, Boos D, Stemmann O. Cleavage of cohesin rings coordinates the separation of centrioles and chromatids. Nat Cell Biol. 2011; 13(8):966–72. [PubMed: 21743463]
32. Yamada HY, Rao CV. Brd8 is a chemosensitizing target for spindle poisons in colorectal cancer therapy. Int J Oncol. 2009; 35:1101–1109. [PubMed: 19787264]
33. Chen J, Elfiky A, Han M, Chen C, Saif MW. The role of Src in colon cancer and its therapeutic implications. Clin Colorectal Cancer. 2014; 13(1):5–13. [PubMed: 24361441]
34. Voisin L, Julien C, Duhamel S, Gopalbhai K, Claveau I, Saba-El-Leil MK, et al. Activation of MEK1 or MEK2 isoform is sufficient to fully transform intestinal epithelial cells and induce the formation of metastatic tumors. BMC Cancer. 2008; 8:337. [PubMed: 19014680]
35. Mermelshtein A, Gerson A, Walfisch S, Delgado B, Shechter-Maor G, Delgado J, et al. Expression of D-type cyclins in colon cancer and in cell lines from colon carcinomas. Br J Cancer. 2005; 93(3):338–45. [PubMed: 16012517]

36. Knüpfer H, Preiss R. Serum interleukin-6 levels in colorectal cancer patients--a summary of published results. Int J Colorectal Dis. 2010; 25(2):135–40. [PubMed: 19898853]
37. Catlett-Falcone R, Landowski TH, Oshiro MM, Turkson J, Levitzki A, Savino R, et al. Constitutive activation of Stat3 signaling confers resistance to apoptosis in human U266 myeloma cells. Immunity. 1999; 10(1):105–15. [PubMed: 10023775]
38. Li Y, de Haar C, Chen M, Deuring J, Gerrits MM, Smits R, et al. Disease-related expression of the IL6/STAT3/SOCS3 signalling pathway in ulcerative colitis and ulcerative colitis-related carcinogenesis. Gut. 2010; 59(2):227–35. [PubMed: 19926618]
39. Lassmann S, Weis R, Makowiec F, Roth J, Danciu M, Hopt U, et al. Array CGH identifies distinct DNA copy number profiles of oncogenes and tumor suppressor genes in chromosomal- and microsatellite-unstable sporadic colorectal carcinomas. J Mol Med (Berl). 2007; 85(3):293–304. [PubMed: 17143621]
40. Li Z, Meng J, Xu TJ, Qin XY, Zhou XD. Sodium selenite induces apoptosis in colon cancer cells via Bax-dependent mitochondrial pathway. Eur Rev Med Pharmacol Sci. 2013; 17(16):2166–71. [PubMed: 23893182]
41. Li Q, Dashwood WM, Zhong X, Nakagama H, Dashwood RH. Bcl-2 overexpression in PhIP-induced colon tumors: cloning of the rat Bcl-2 promoter and characterization of a pathway involving beta-catenin, c-Myc and E2F1. Oncogene. 2007; 26(42):6194–202. [PubMed: 17404573]
42. Janssen A, van der Burg M, Szuhai K, Kops GJ, Medema RH. Chromosome segregation errors as a cause of DNA damage and structural chromosome aberrations. Science. 2011; 333:1895–1898. [PubMed: 21960636]
43. Crasta K, Ganem NJ, Dagher R, Lantermann AB, Ivanova EV, Pan Y, et al. DNA breaks and chromosome pulverization from errors in mitosis. Nature. 2012; 482:53–58. [PubMed: 22258507]
44. Mallardo M, Giordano V, Dragonetti E, Scala G, Quinto I. DNA damaging agents increase the stability of interleukin-1 alpha, interleukin-1 beta, and interleukin-6 transcripts and the production of the relative proteins. J Biol Chem. 1994; 269(21):14899–904. [PubMed: 8195120]
45. Nagasaki T, Hara M, Nakanishi H, Takahashi H, Sato M, Takeyama H. Interleukin-6 released by colon cancer-associated fibroblasts is critical for tumour angiogenesis: anti-interleukin-6 receptor antibody suppressed angiogenesis and inhibited tumour-stroma interaction. Br J Cancer. 2014; 110(2):469–78. [PubMed: 24346288]
46. Herman JG, Merlo A, Mao L, Lapidus RG, Issa JP, Davidson NE, et al. Inactivation of the CDKN2/p16/MTS1 gene is frequently associated with aberrant DNA methylation in all common human cancers. Cancer Res. 1995; 55(20):4525–30. [PubMed: 7553621]
47. Okamoto A, Demetrick DJ, Spillare EA, Hagiwara K, Hussain SP, Bennett WP, et al. Mutations and altered expression of p16INK4 in human cancer. Proc Natl Acad Sci U S A. 1994; 91(23): 11045–9. [PubMed: 7972006]
48. Baker DJ, Jeganathan KB, Cameron JD, Thompson M, Juneja S, Kopecka A, et al. BubR1 insufficiency causes early onset of aging-associated phenotypes and infertility in mice. Nat Genet. 2004; 36(7):744–9. [PubMed: 15208629]
49. Baker DJ, Wijshake T, Tchkonia T, LeBrasseur NK, Childs BG, van de Sluis B, et al. Clearance of p16Ink4a-positive senescent cells delays ageing-associated disorders. Nature. 2011; 479(7372): 232–6. [PubMed: 22048312]
50. Weaver BA, Silk AD, Montagna C, Verdier-Pinard P, Cleveland DW. Aneuploidy acts both oncogenically and as a tumor suppressor. Cancer Cell. 2007; 11(1):25–36. [PubMed: 17189716]

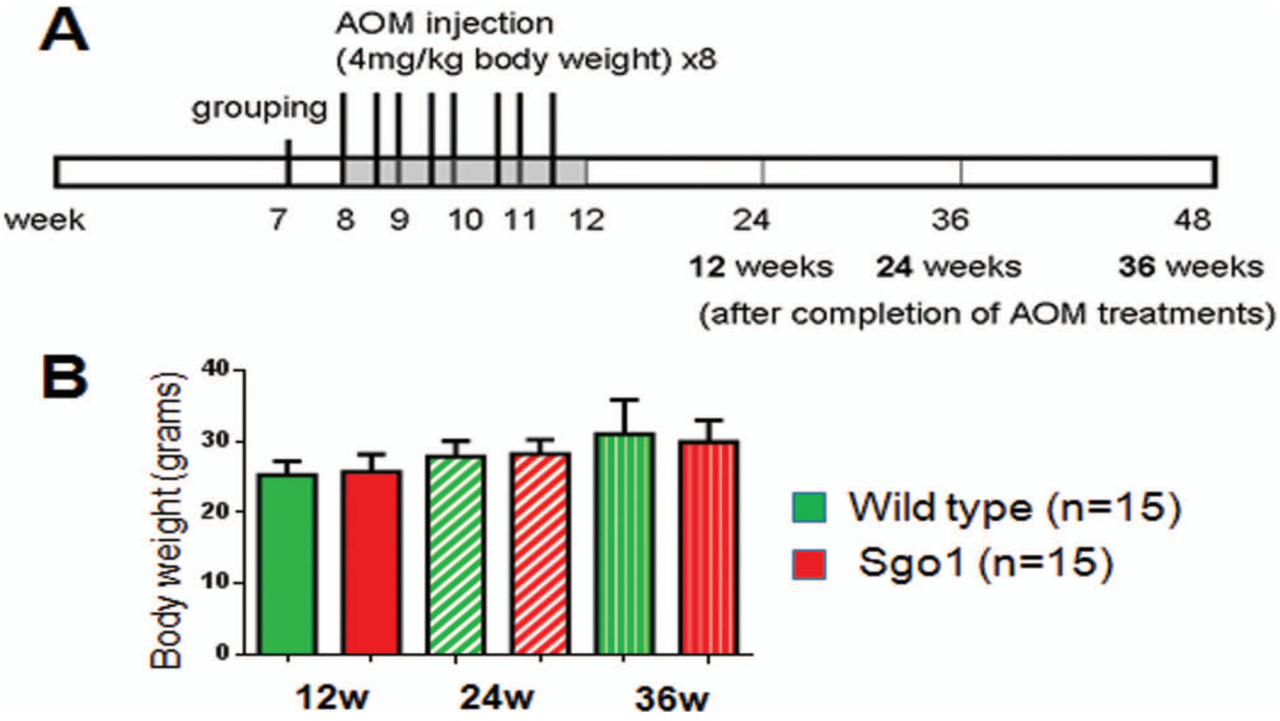

Fig 1. Experimental scheme

(A) Samples were collected at three endpoints (12 weeks, 24 weeks, and 36 weeks post AOM treatments). For gross tumor formation, see Table 1. Only limited and comparable numbers of colon tumors developed at the endpoints. No loss of animals was observed during the entire experiment. (B) Average body weight at each endpoint showed no statistically significant difference. *N*=15 for wild-type (green) and for Sgo1 (red).

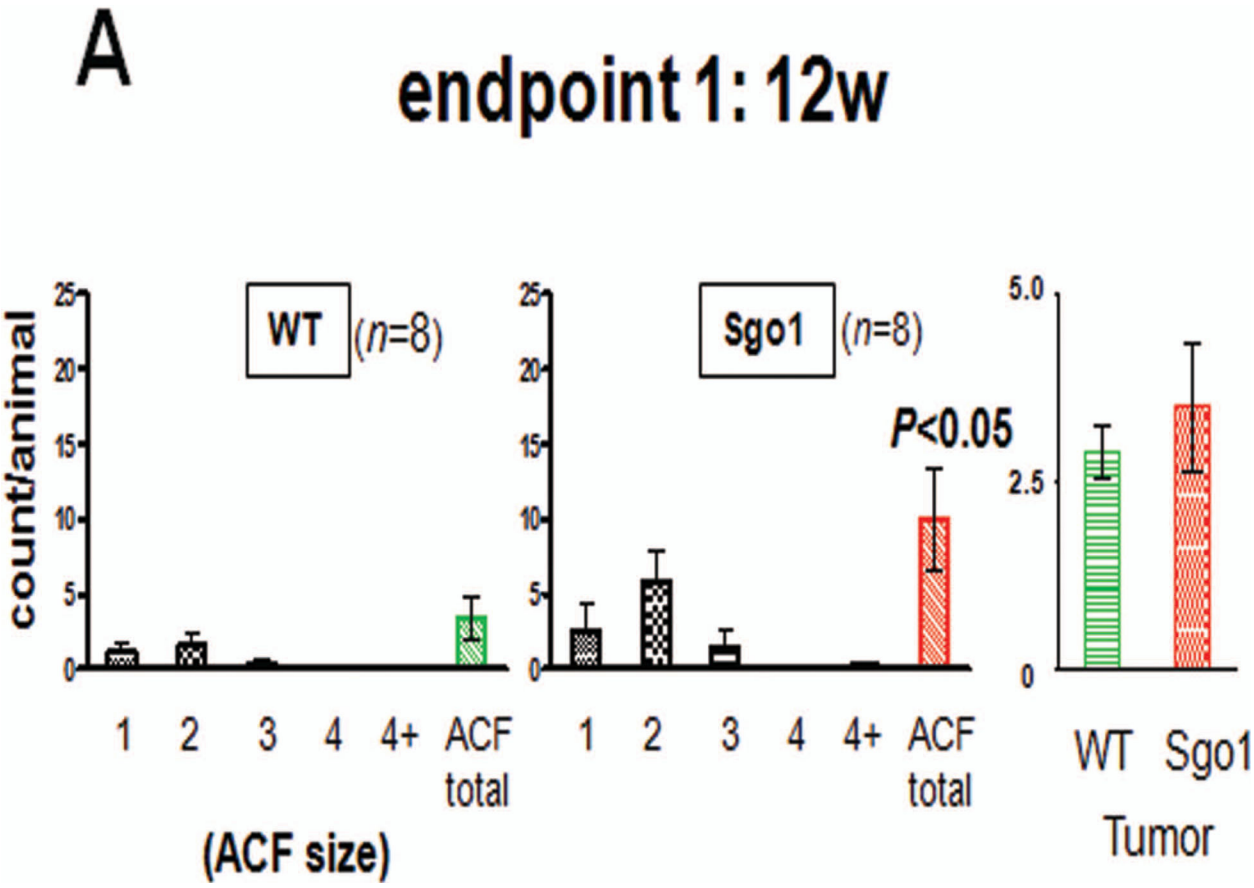

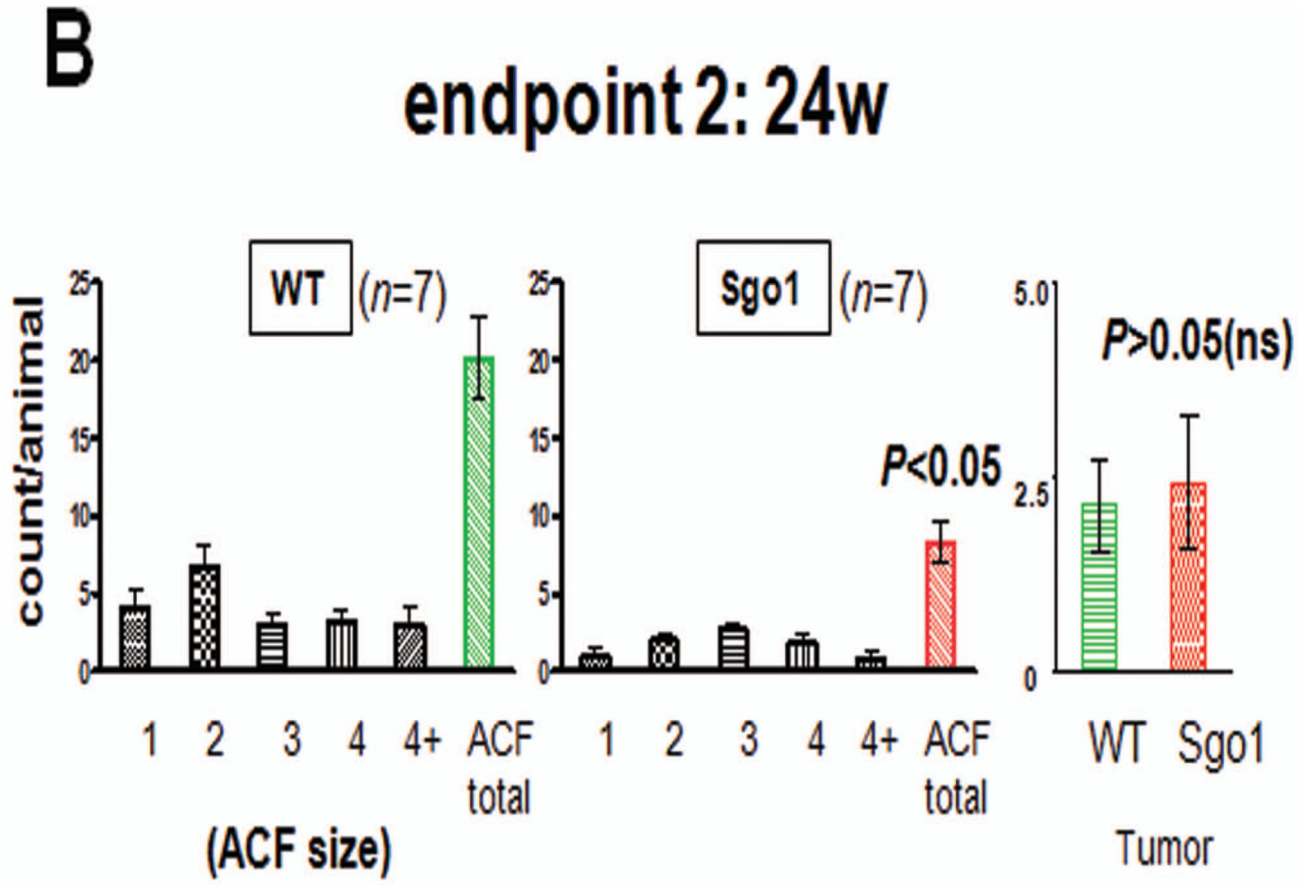

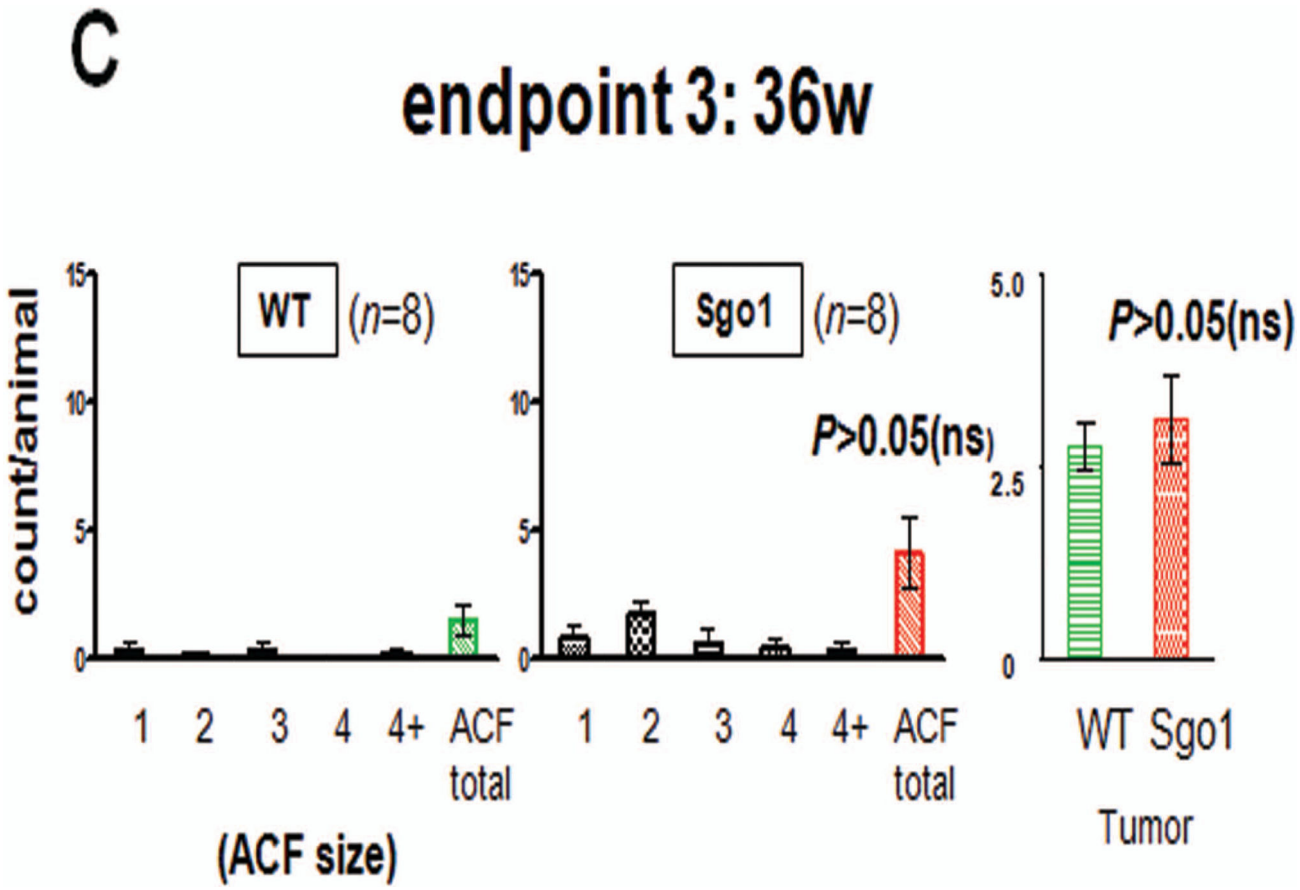

Fig2. Different dynamics in the development of colonic ACFs and tumors (microadenomas) in wild-type and Sgo1 mice

(A) At endpoint 1 (12 weeks), the total ACF number per animal was significantly higher in Sgo1 mice, indicating rapid development of lesions in Sgo1. (B) At endpoint 2 (24 weeks), wild-type mice kept developing ACF, yet further development of ACF in Sgo1 mice was not observed. The total ACF number per animal was significantly less in Sgo1 mice. Numbers of microscopic tumors (microadenomas) showed no difference (ns: non-significant). (C) At endpoint 3 (36 weeks), most ACF regressed in both strains.

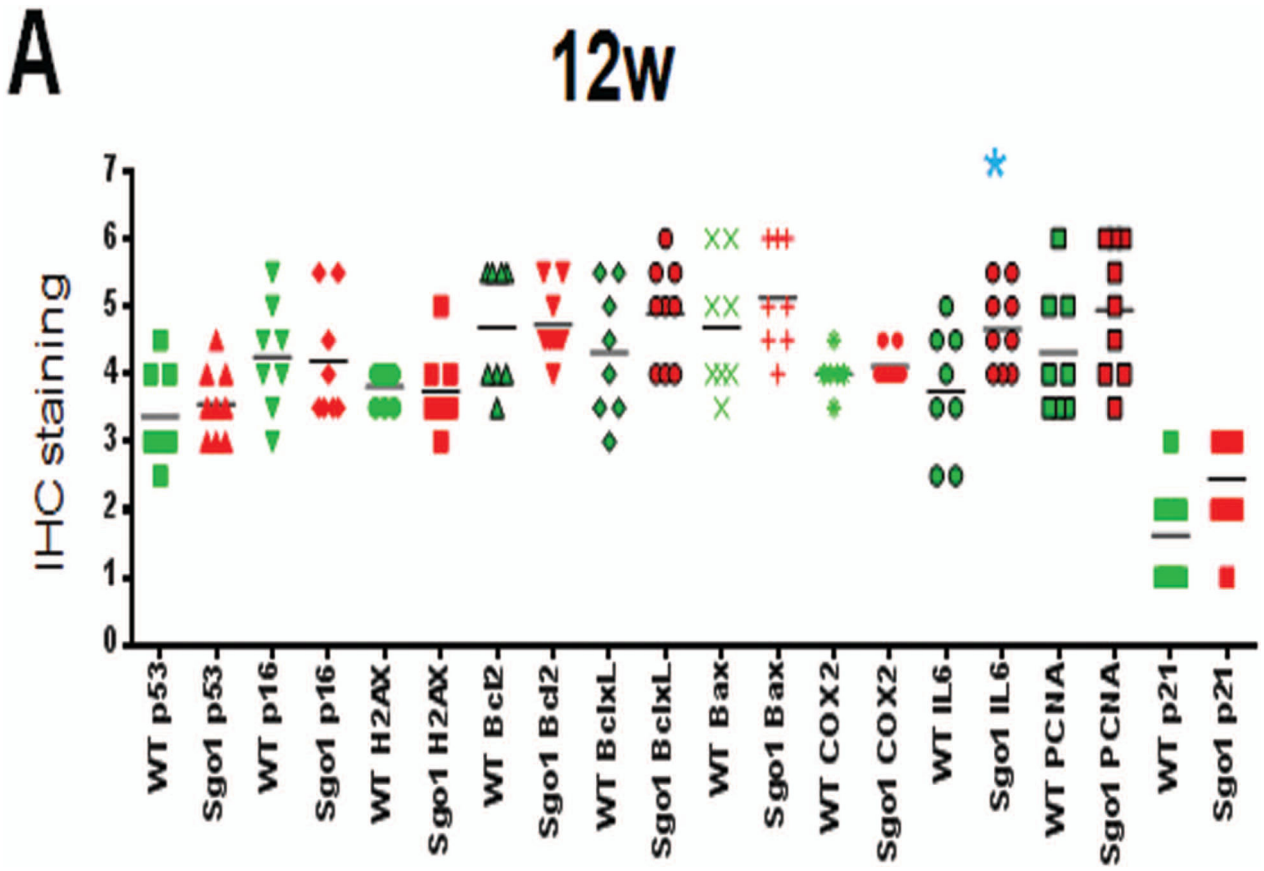

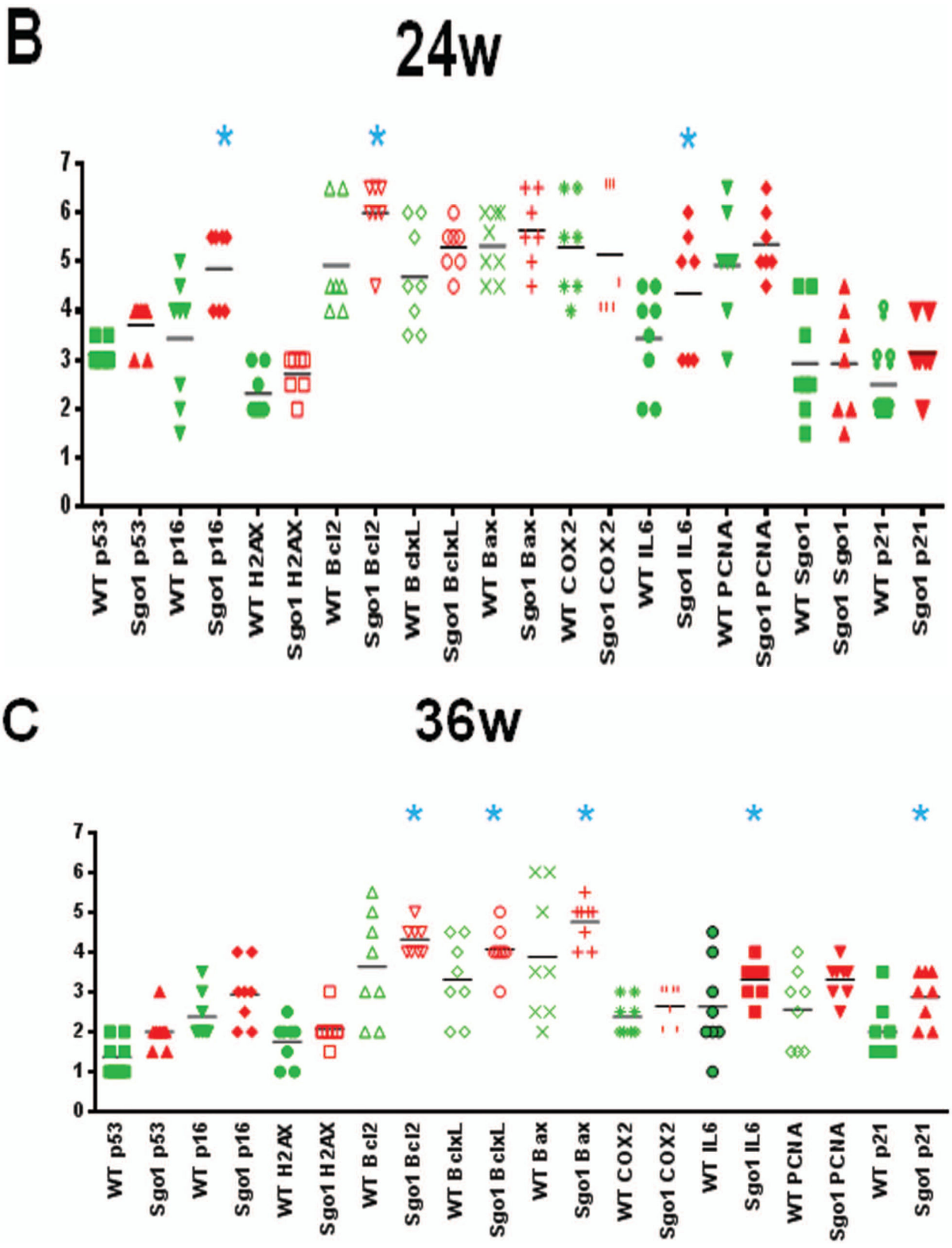

Fig3. Differentially expressed proteins in Sgo1 colon

Paraffin-embedded colon sections were stained with the indicated antibody. Samples from wild-type mice are indicated in green, Sgo1 mice in red. IHC signals were graded in 7 grades (See Materials and Methods) for indicated markers. Asterisk (blue) indicates more than 1 grade scale difference in expression. (A) 12 weeks endpoint. IL-6 was expressed notably higher in Sgo1 mice. (B) 24 weeks endpoint. p16, Bcl2, and IL-6 were notably higher in Sgo1 mice. (C) 36 weeks endpoint. Bcl2, BclxL, Bax, IL-6, and p21 were notably higher in Sgo1 mice.

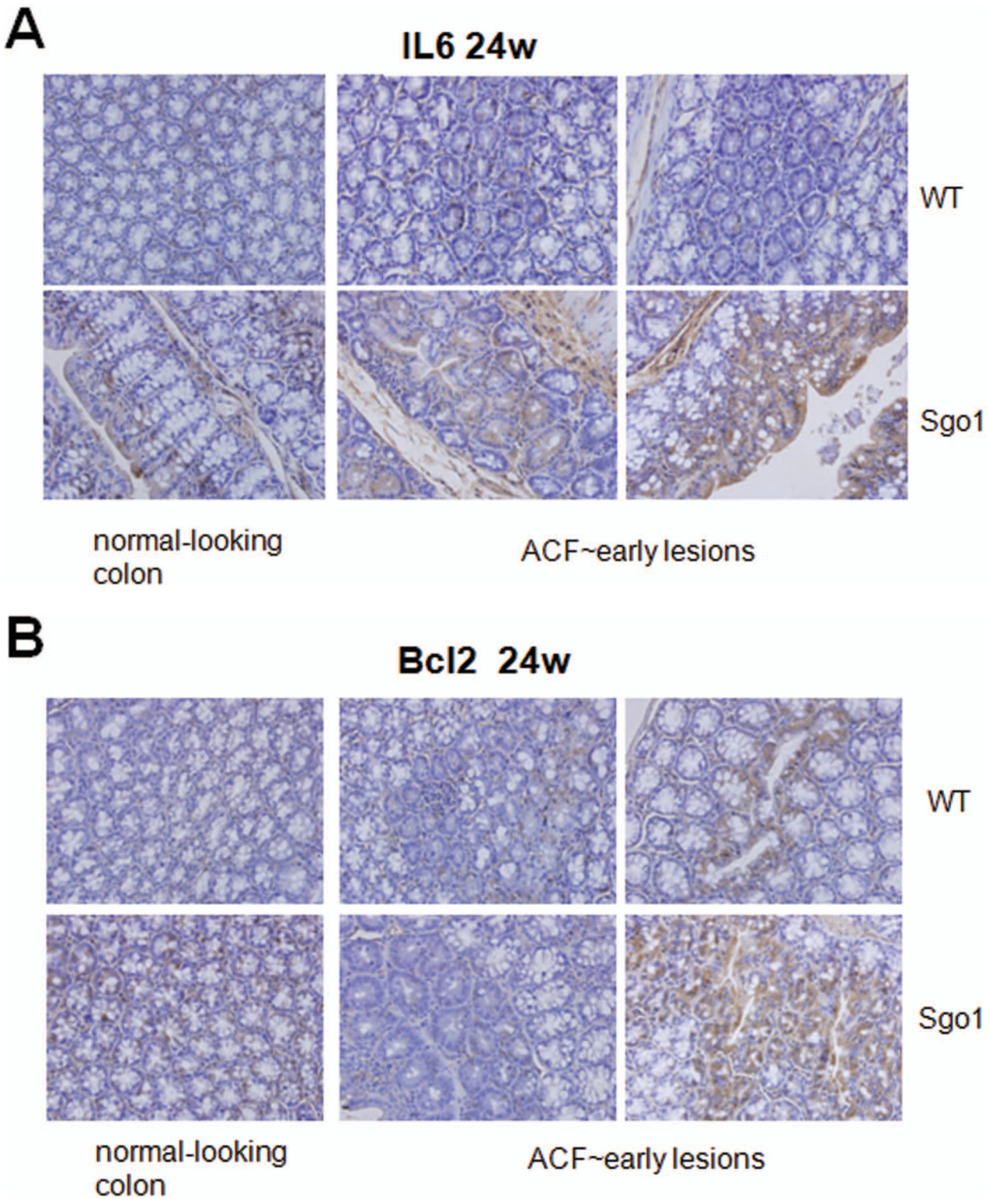

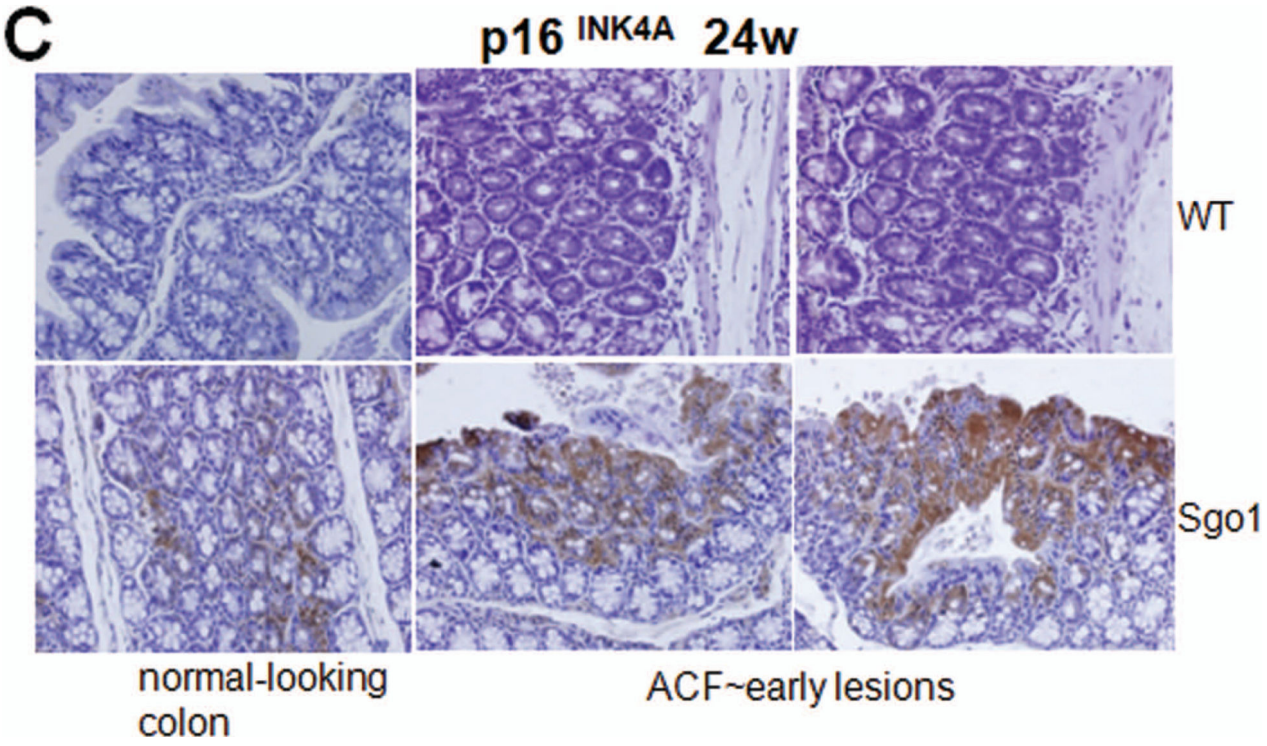

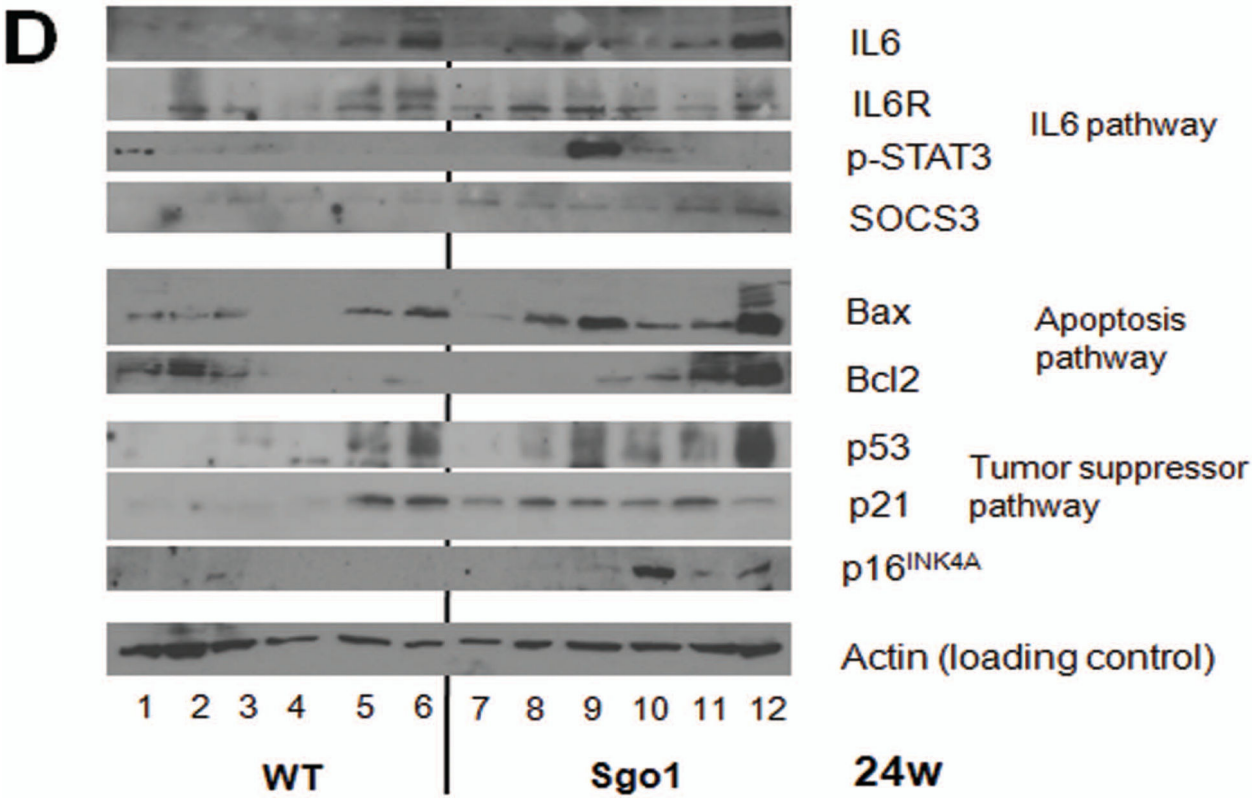

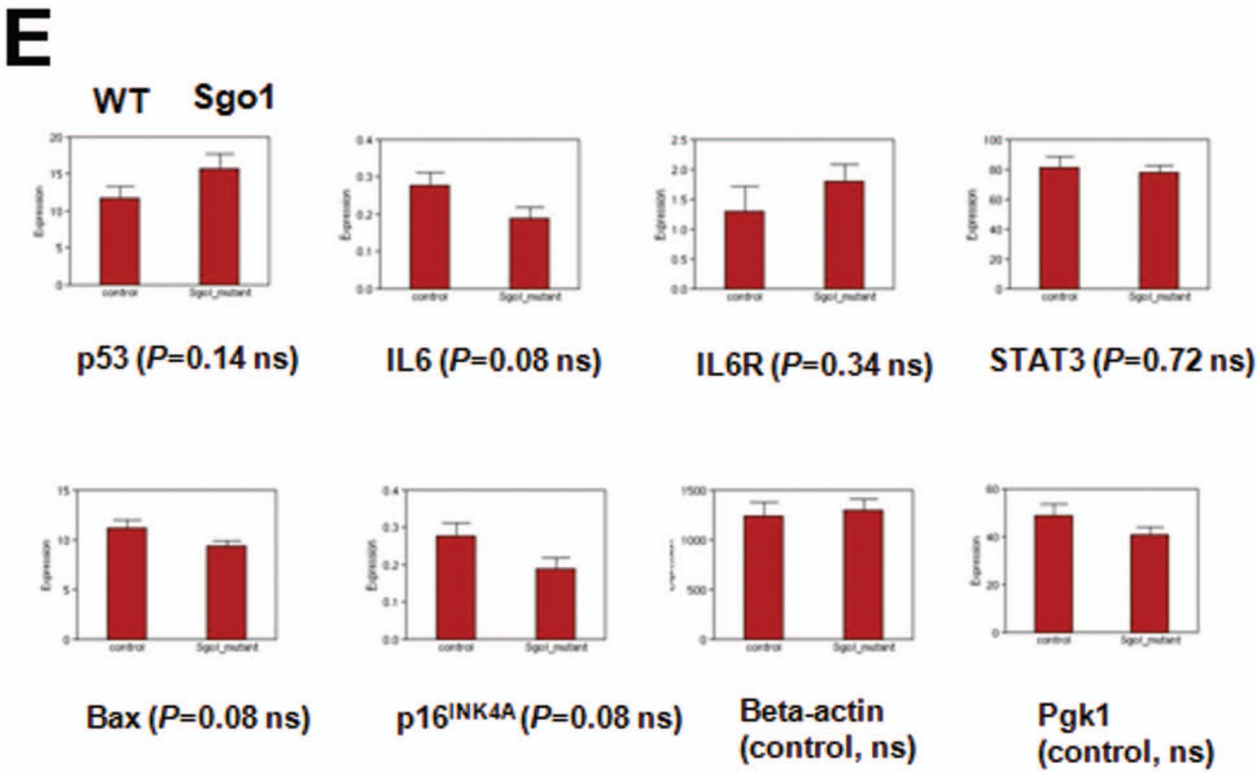

Fig 4. Different patterns of IL-6, Bcl2, and p16^{INK4A} protein localization in wild-type and Sgo1 mice

(A) IL-6 expression was generally low in normal-looking mucosa in Sgo1$^{-/+}$ and wild-type controls. Lesions in wild-type mice sporadically showed IL-6-positive cells. The signals were prominent in lesions in Sgo1$^{-/+}$. (B) Bcl2 expression was higher in normal-looking parts of colons in Sgo1$^{-/+}$ mice than in wild-type mice. As lesions developed, Bcl2 expression increased in both Sgo1$^{-/+}$ and wild-type mice. (C) p16^{INK4A} expression was low in wild-type mice, but higher in Sgo1$^{-/+}$ mice, in both normal-looking colons and in lesions. [(A)-(C): all ACF/lesions were confirmed by a histopathologist]. (D) Immunoblots for the markers; IL6/STAT3/SOCS3 pathway (IL6, IL6 receptor (IL6R), phosphor-STAT3, SOCS3), apoptosis pathway (Bcl2, Bax), tumor suppressor pathway (p53, p21, p16^{INK4A}). Samples from Sgo1 (lanes 7-12) tend to show an increase in marker protein expression compared with samples from wild type (lanes 1-6), in agreement with IHC results. (E) The differences in protein amount may not be due to transcriptional upregulation. NGS readouts (left bar: wild type; right bar: Sgo1) did not show significant up-regulation in mRNA level for indicated markers. Beta-actin and pgk1 (Phosphoglycerate kinase 1) are commonly used for qPCR controls. The readouts are shown as NGS quantification controls. ns: non-significant.

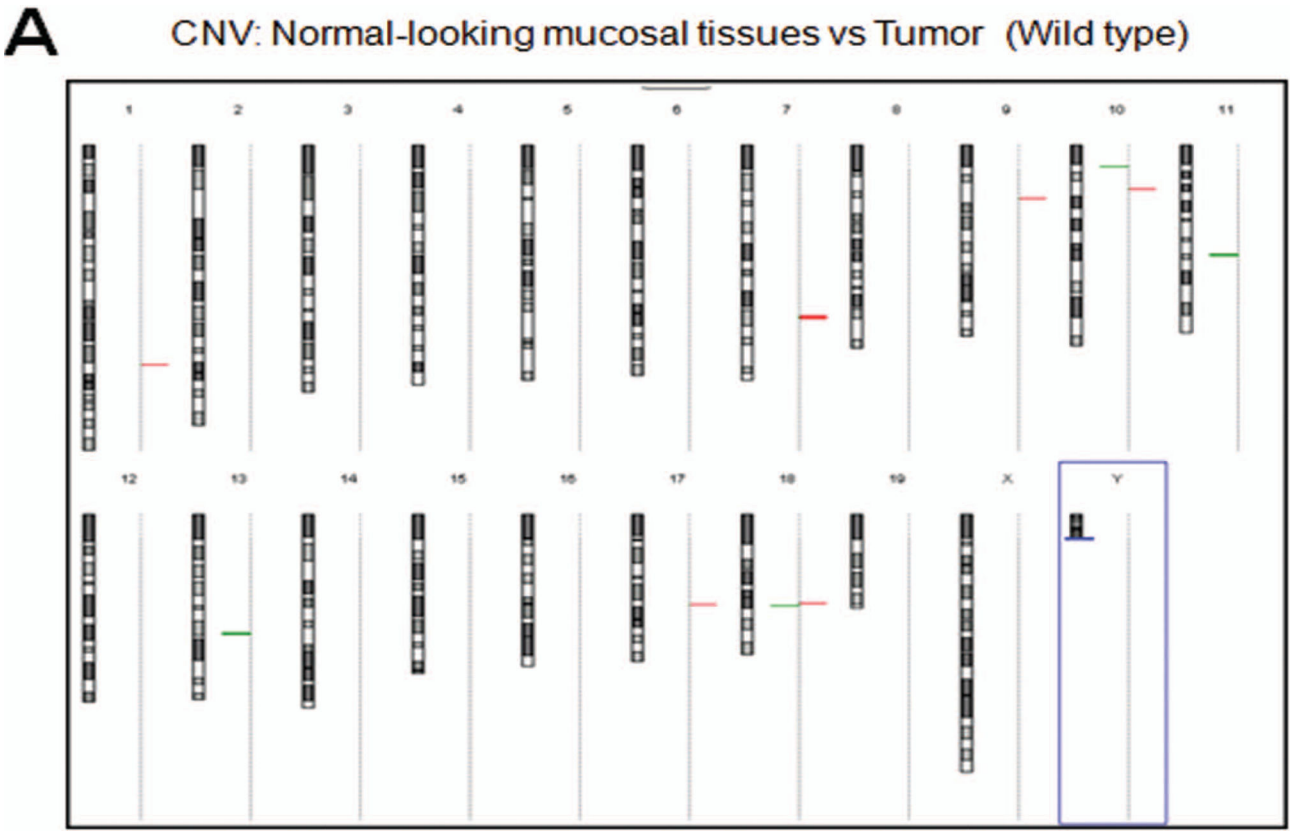

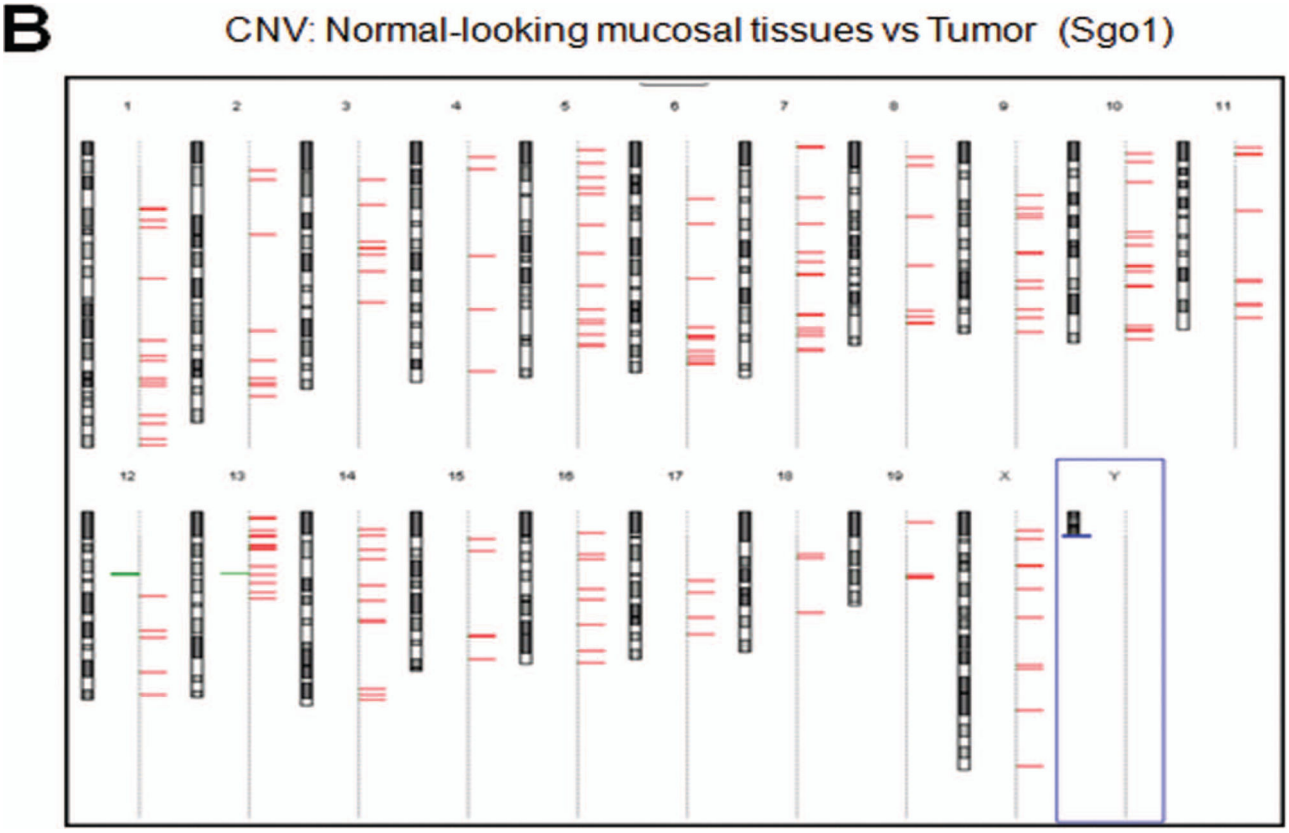

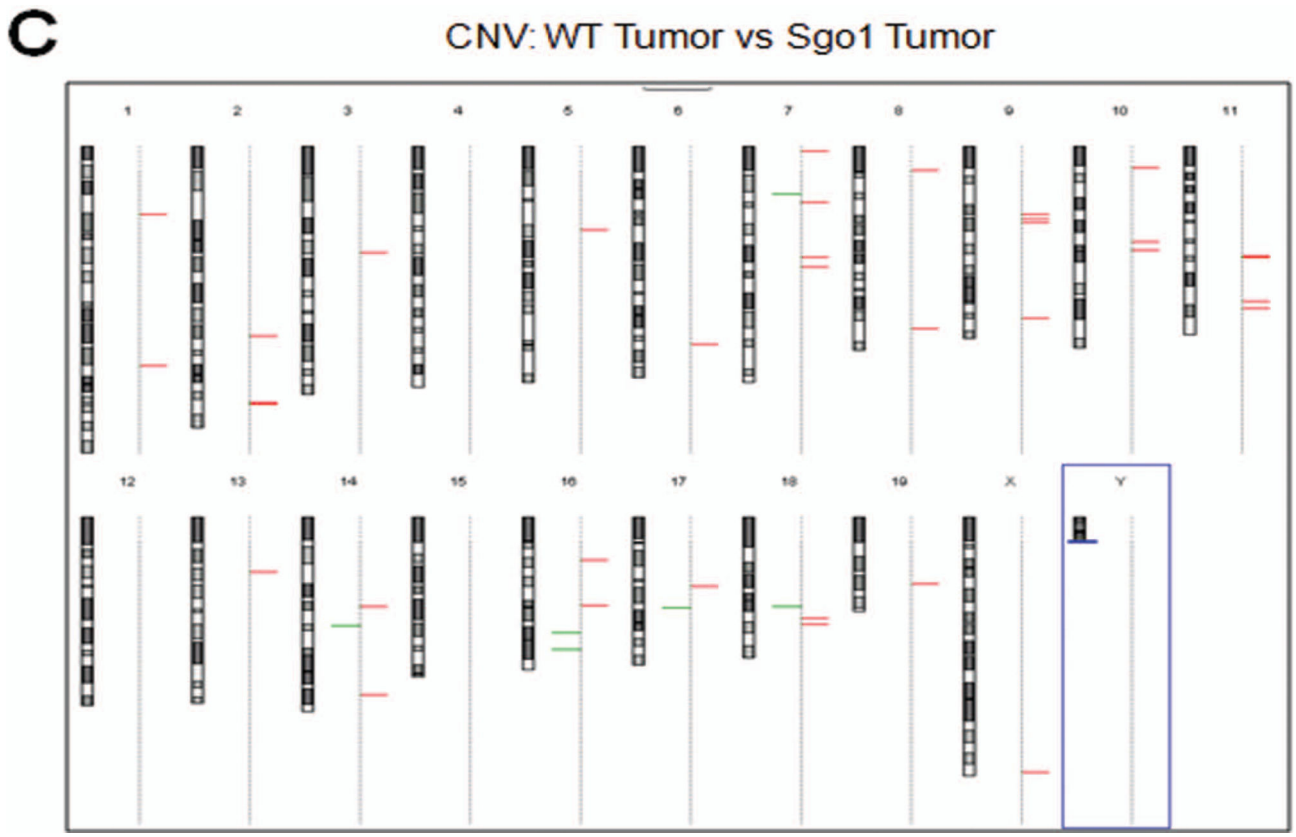

Fig 5. Tumors in Sgo1 mice had higher CNV than tumors in wild-type mice

(A) Normal-looking mucosal tissues vs tumors [wild-type]. 12 CNV were identified in the tumor. Red: amplification. Green: loss. (B) Normal-looking mucosal tissues vs tumors [Sgo1]. 165 CNV were identified in the tumor. (C) Wild-type tumors vs Sgo1 tumors. 40 CNV were identified. The CNV analysis was array/hybridization-based, and would detect regional loss/gain in chromosomes as well as whole chromosome loss/gain if happened in a majority of the tumor cells. However, it should be noted that polyploidization (e.g. tertaploidization) may not be detected well in this method. Since we used female mice for the experiments, no Y chromosome probes appeared positive in this analysis.

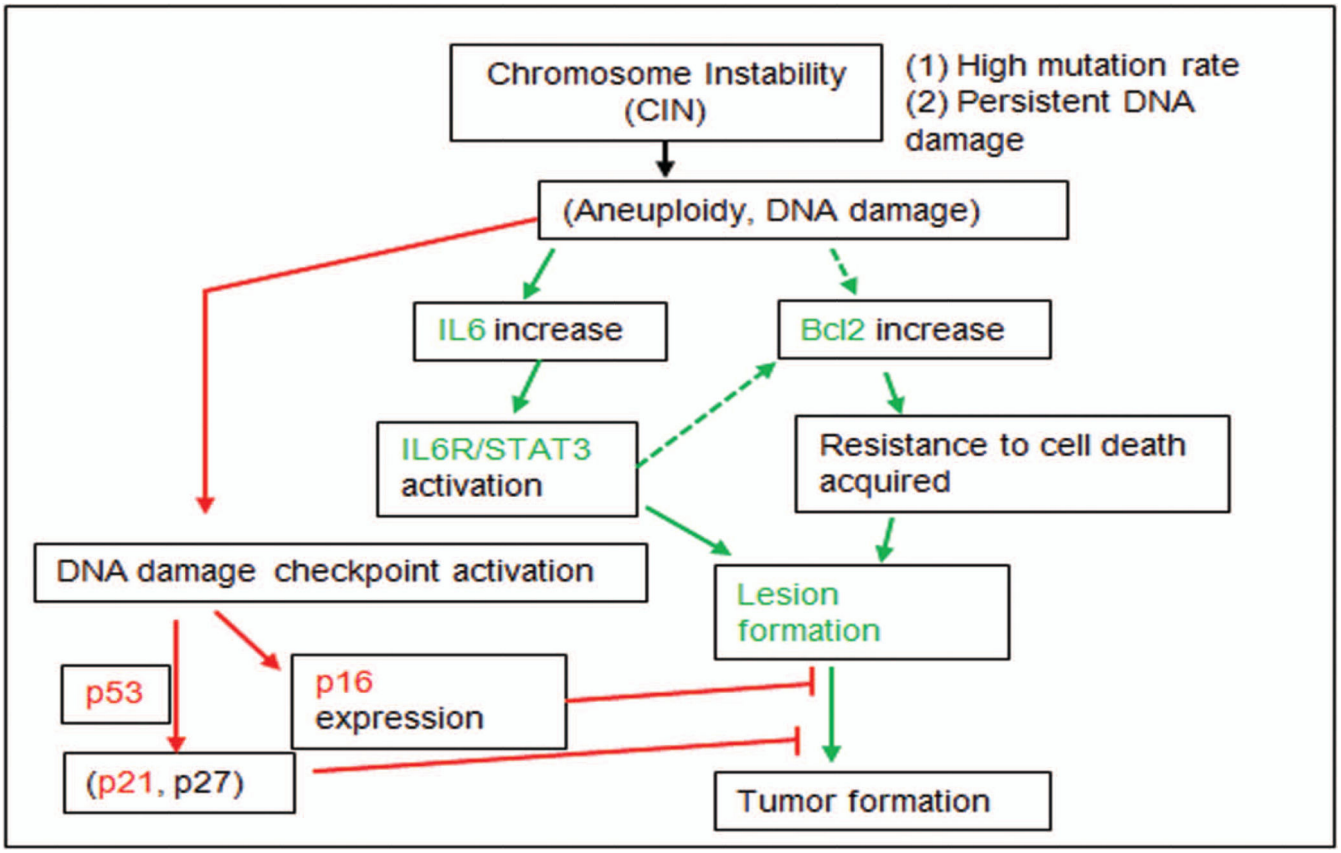

Fig 6. Model for differential dynamics in lesion/tumor development with Sgo1 defects

Current hypothetical model for how Sgo1 defect-mediated CIN leads to differential dynamics in colon lesion and tumor development. CIN leads to a high mutation rate and DNA damage, resulting in aneuploidy and/or DNA damage (16, 42, 43). As a result, the DNA damage checkpoint is activated and senescence is induced. The senescence serves to inhibit lesion/tumor growth. On the other hand, DNA damage leads to activation of IL-6 pathway. In addition, the Bcl2/Bax/BclxL-mediated cell death pathway is affected and a resistance to cell death is acquired. These two events drive initial lesion and tumor formation. The differential dynamics in the high CIN condition are a result of these antagonizing pathways. Formation process of tumors with high CIN may be modulated by interventions in these pathways.

Table 1

Gross observation and tumor formation at each endpoint

Endpoint	strain	n	Gross observation
1 (12w post AOM)	Wild-Type	15	Normal 15
	Sgol	15	Normal 13, colon tumor 2
2 (24w post AOM)	Wild-Type	15	Normal 11, liver tumor 1, lung tumor 1, colon tumor 2
	Sgol	15	Normal 11, cirrhotic liver 1, ovary cyst 1, colon tumor 2
3 (36w post AOM)	Wild-Type	15	Normal 7, obese 3, liver tumor 2, lung tumor 1, GI tumor 1, colon tumor 1
	Sgol	15	Normal 11, obese 1, liver and colon tumor 1, liver cyst 1, ovary tumor 1

There was no difference in the numbers of gross (visually identifiable) tumors between wild-type and Sgo1−/+ mice.